ISSN 1069-3513, Izvestiya, Physics of the Solid Earth, 2014, Vol. 50, No. 6, pp. 795–813. © Pleiades Publishing, Ltd., 2014.
Original Russian Text © K.Zh. Seminsky, A.A. Bobrov, S. Demberel, 2014, published in Fizika Zemli, 2014, No. 6, pp. 80–98.

Variations in Radon Activity in the Crustal Fault Zones: Spatial Characteristics

K. Zh. Seminsky, A. A. Bobrov, and S. Demberel

Institute of the Earth's Crust, Siberian Branch of the Russian Academy of Sciences, ul. Lermontova 128, Irkutsk, 664033 Russia

Research Center for Astronomy and Geophysics, Academy of Sciences of Mongolia, Ulan Bator, Mongolia

e-mail: seminsky@crust.irk.ru, alexbob@crust.irk.ru, demberel@rcag.ac.mn

Received: August 19, 2013

Abstract—The data of the profile gas emanation survey conducted on three spatial scales in separate regions of the Mongolia–Baikal seismic belt are generalized to establish the regularities of the spatially heterogeneous distribution of soil radon activity above the active faults in the Earth's crust. It is shown that the shapes, sizes, and contrast of the near-fault radon anomalies are complicated by erosion and weathering; however, the critical role in their formation is played by the structural–geological controls, which determine the internal structure and recent activity of the fault zones. As a consequence, the cross-fault shape of the studied radon anomalies is vitally controlled by four structural situations, which correspond to the combinations of the structural type of the fault (localized/distributed) and the presence/absence of the fine filler material in the zone controlled by the fault. The cross-fault dimension of the emanation anomaly is commensurate or slightly larger than the width of the fault zone comprising all the fractures and joints associated with the formation of the main fault, which, due to the low permeability of the tectonites, is in most cases marked by the lowest concentration of soil radon. The contrast of the emanation anomalies, which we suggest to estimate in terms of a relative parameter K_Q, gravitates to certain levels of this parameter. This provides the basis for distinguishing five groups of the fault zones with low ($K_Q \leq 2$), moderate ($2 < K_Q \leq 3$), increased ($3 < K_Q \leq 5$), high ($5 < K_Q \leq 10$), and ultrahigh ($K_Q > 10$) radon activity. The previous studies show that for increasing the efficiency of the emanation survey in the fault zones, it is advisable to set up long profiles, reduce the measurement step in the vicinities of the main faults, specify the threshold of identifying the anomalies at the arithmetic mean level over the profile, and use the relative parameter K_Q for comparing and estimating the faults in terms of the intensity of their radon activity.

DOI: 10.1134/S1069351314060081

INTRODUCTION

The emanation survey has been traditionally thought of as a suitable tool for identifying the blind faults which are hidden beneath the overburden but are currently permeable for the underground gases. Moreover, the level of radon concentration in soil air is in some cases believed to be directly related to the intensity of the contemporary geodynamical activity of the faults. Indeed, according to the previous data of many authors, the faults are accompanied by the radon anomalies having a simple shape with the maximum in the activity of soil radon (Q, Bq/m^3) above the main fault and minimal concentrations on the fault's margins (Ioannides et al., 2003; Moussa and El Arabi, 2003; Font et al., 2008, etc.). At the same time, with the accumulation of experience in the emanation studies, it has become clear that the anomalies above the tectonic dislocations widely vary in intensities and shapes as do their positions within the main fault (Duddridge et al., 1991; King et al., 1993; Toutain and Baubron, 1999; Atallah et al., 2001; Al-Bataina et al., 2005; Inceöz et al., 2006; Wiersberg and Erzinger, 2008; Richon et al., 2010). Thus, for the new level of research, it was required to analyze the source of this diversity from the standpoint of the modern understanding of the fault structure.

In this context, it is critically important that the term "fault zone" is understood in a wide tectonophysical sense, according to which this object includes, in addition to the tectonites of the main fault, also the significantly larger volumes of the rocks which have undergone plastic and fracture deformations genetically related to the formation of the main fault. Even in the conditions of a stable (constant) tectonic regime, the evolution of the fault zones is dominated by the initial spatiotemporal heterogeneity (Seminsky, 2003), which results in the stepwise development and naturally irregular pattern of fracturing of the substrate of the fault zones across and along their strike with alternating segments with denser and rarer faults. The disjunctives arising at different stages of the evolution strongly differ by their structure. At the early stages, there are a few large active faults in the fault zone (the distributed fault), whereas at the final stages the zone is largely dominated by a single main fault (localized fault).

Even apart from the time variations in the radon field, whose allowance presents a separate problem, the described structural features of the fault zones and their diverse geodynamic activity (Rikitake, 1978; Voitov, 1998; Toutain and Baubron, 1999; Cicerone et al., 2009; Spivak, 2010; Utkin et al., 2010; Adushkin et al., 2012, etc.) predetermine the existence of radon anomalies with various intensity and shapes associated with these tectonic structures. This conclusion for separate objects was supported by the results of the profile emanation survey carried out for a few dozens of faults in the south of East Siberia and Mongolia (Seminsky and Bobrov, 2009a; Seminsky and Demberel, 2013). In the present study, we intended to generalize the results of emanation studies at the different-rank faults of the Mongolia–Baikal seismic belt based on the tectonophysical approach and to identify the key regularities in the distribution of radon activity in these structures. For doing this, it was required to (1) assess the role of the structural-geological factors in the formation of the radon field above the fault zones, (2) typify the structural situations determining the pattern of the near-fault radon anomalies, and (3) reveal the levels of radon activity that objectively exist for the faults in the studied region.

THE OBJECTS OF STUDY AND THE SCALE LEVELS OF EMANATION STUDIES

Within the Baikal-Mongolian seismic belt, which is associated with the area of young orogeny in the south of Siberia and Mongolia, the emanation surveys were localized in two regions characterized by diverse landscape and weather conditions and different geodynamical regimes of crustal evolution at the present stage of tectogenesis. The Baikal zone of lithospheric extension was studied with a different degree of detail along the 250-km Bayandai–Tarbagatai transect (Fig. 1a), which cuts the shoulders of the Baikal rift accommodating the interaction of the Siberian and Transbaikalian lithospheric blocks. Despite the dense concentration of the population in the Baikal region, high seismicity, and the regime of crustal extension which is favorable for the seepage of natural gases (Kemski et al., 1996; Atallah et al., 2001; Ioannides et al., 2003; Al-Bataina et al., 2005; Angelone et al., 2005; Tansi et al., 2005; Font et al., 2008; Koike et al., 2009; Richon et al., 2010), this territory is still insufficiently studied in terms of radon activity. The works of B.P. Chernyago et al. (2008; 2012), who revealed the correlation between the indoor values of parameter Q in the houses at some localities in the Baikal region and the radon concentration in the soils, identified the anomalous areas related to the radioactive rocks, and supported the leading role of the faults in the formation of the peak concentrations of soil radon. The estimates of Q above some large faults of the Baikal Rift are made in (Koval et al., 2006) and in our previous papers (Seminsky and Bobrov, 2009a; 2009b). These estimates, within the necessary volume, are used below for a more complete characterization of the near-fault anomalies. The second region of our emanation study comprised Central Mongolia (Fig. 1b) with its sharp continental climate and geodynamical predominance of the regime of crustal shearing, as suggested by the focal mechanisms of the strong earthquakes (*Focal*..., 2011) and other data. Despite the rather high seismicity (Adiya et al., 2003) and the presence of local areas with a dense population, e.g., the city of Ulan Bator accommodates nearly half of the population of Mongolia, the radon activity of the faults in Central Mongolia had not been studied before our dedicated studies (Seminsky and Demberel, 2013).

For solving the stated problems, we used the data of the profile emanation survey carried out on three spatial scales, which generally correspond to the three ranks of the studied disjunctive structures: the fault systems, the large and the small fault zones. The complete hierarchy of the faults was investigated for the region of crustal extension (Fig. 1a), where, according to the existing definition (Park, 1997) and nomenclature of the main faults (*Karta*..., 1982; Mats, 1993; San'kov et al., 1997), the fault systems comprise the Obruchev (I), Chersky–Barguzin (II), and Dzhida–Vitim (III) tectonic structures. These structures were cut by two segments of the Bayandai–Krestovskii and Kudara–Tarbagatai transect, along which the parameter Q was measured with a step of ~2500 m.

In the opinion of most researchers (Mats, 1993; Delvaux et al., 1997), the Obruchev fault system, which was the main object of the emanation studies, has two normal-fault branches in the Central Baikal region: the Primorskaya branch running inland in the Olkhon region and the Morskaya (Olkhon) branch located on the submarine slope of Lake Baikal (Fig. 2). The Primorskaya fault zone, expressed in the topography by the Buguldei–Chernorudskii graben (Dombrovskaya, 1973; Mats, 1993) is related to the tectonic type of the large rift-forming normal faults; it was studied within the 5-km segment of the Bayandai–Krestovskii profile (11.5–16.5 km) with an interval of Q-parameter measurements of 250 m (Fig. 3).

The detailed emanation survey with a step of 20–25 m and less (up to every 2.5–5 m) in the vicinity of the main fault was used for studying the radon field above the faults which are clearly expressed by the characteristic scarps in the topography of the terrain and by loose tectonites in the outcrops of the hard rocks. The rift objects are located in the Olkhon region, which belongs to the Obruchev fault system and is confined between the Primorskii and Morskoi normal faults (Fig. 1a). Here, the detailed studies have been carried out for the Primorskii fault in the region of the Sarma paleoseismodislocation (Khromovskikh, 1965) and the Ulirbin, Tyrgan-Kuchelgin, Kurkut,

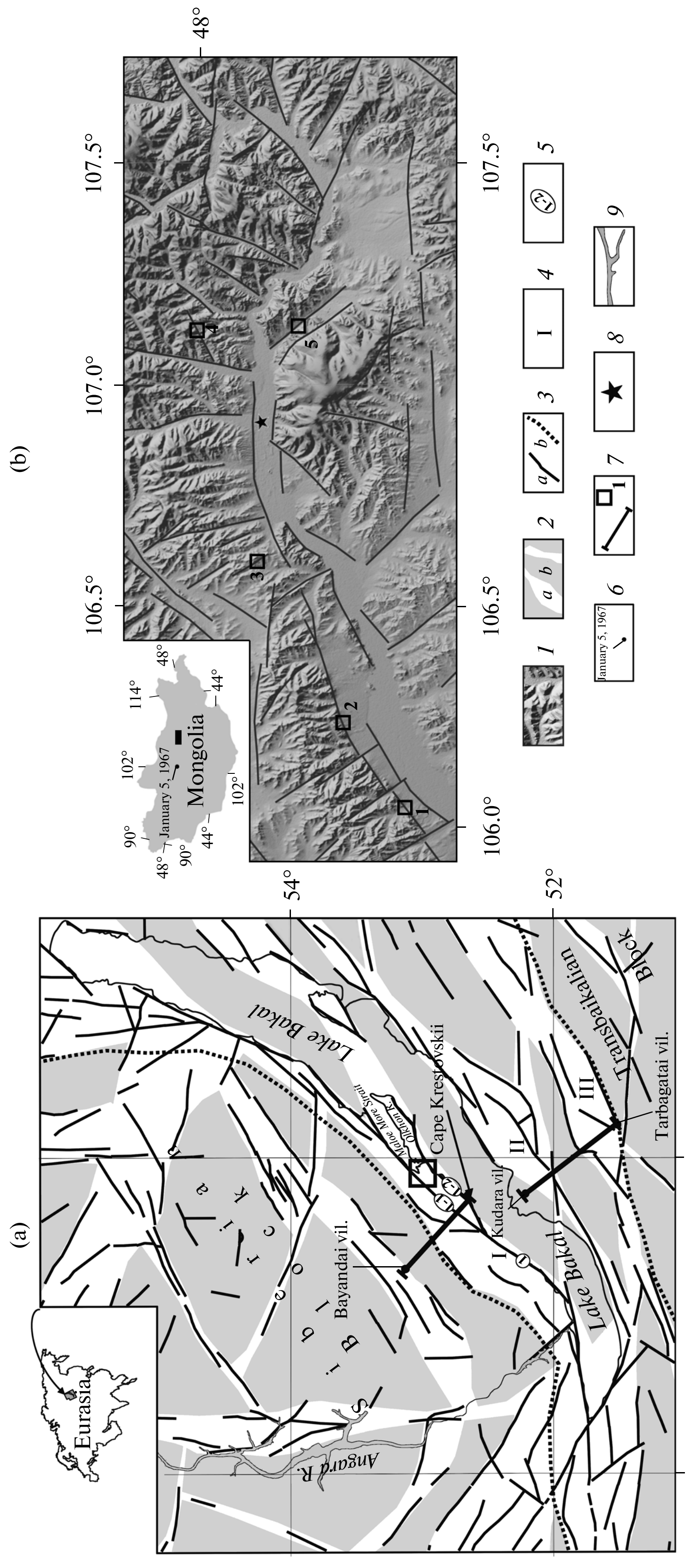

Fig. 1. The layout of the main faults and the areas of the profile emanation surveys in the (a) Baikal region and (b) Central Mongolia. (*1*) The three-dimensional (3D) elevation model in the vicinity of Ulan Bator in Mongolia (the square in the inset); (*2*) the zones with a higher density of the faults (*a*) among the less fractured blocks (b) in the Baikal region; (*3*) the faults expressed by the scarps in the topography (a) and the boundaries of the Baikal Rift (*b*) according to (Seminsky et al., 2013); (*4*) the indices of the fault systems of crustal extension: I, Obruchev; II, Chersky–Barguzin; III, Dzhida–Vitim; (*5*), the indices of the main faults of the Obruchev system: 1, Obruchev fault itself; 1–1, Primorskii; 1–2, Morskoi; (*6*) the epicenter of the Mogod earthquake ($M = 7.8$; January 5, 1967); (*7*) the positions of the Bayanday–Krestovskii and Kudara–Tarbagatai profiles and the segment in the Oklhon region covered by the studies of radon activity; (*8*) Ulan Bator downtown; and (*9*) drainage system.

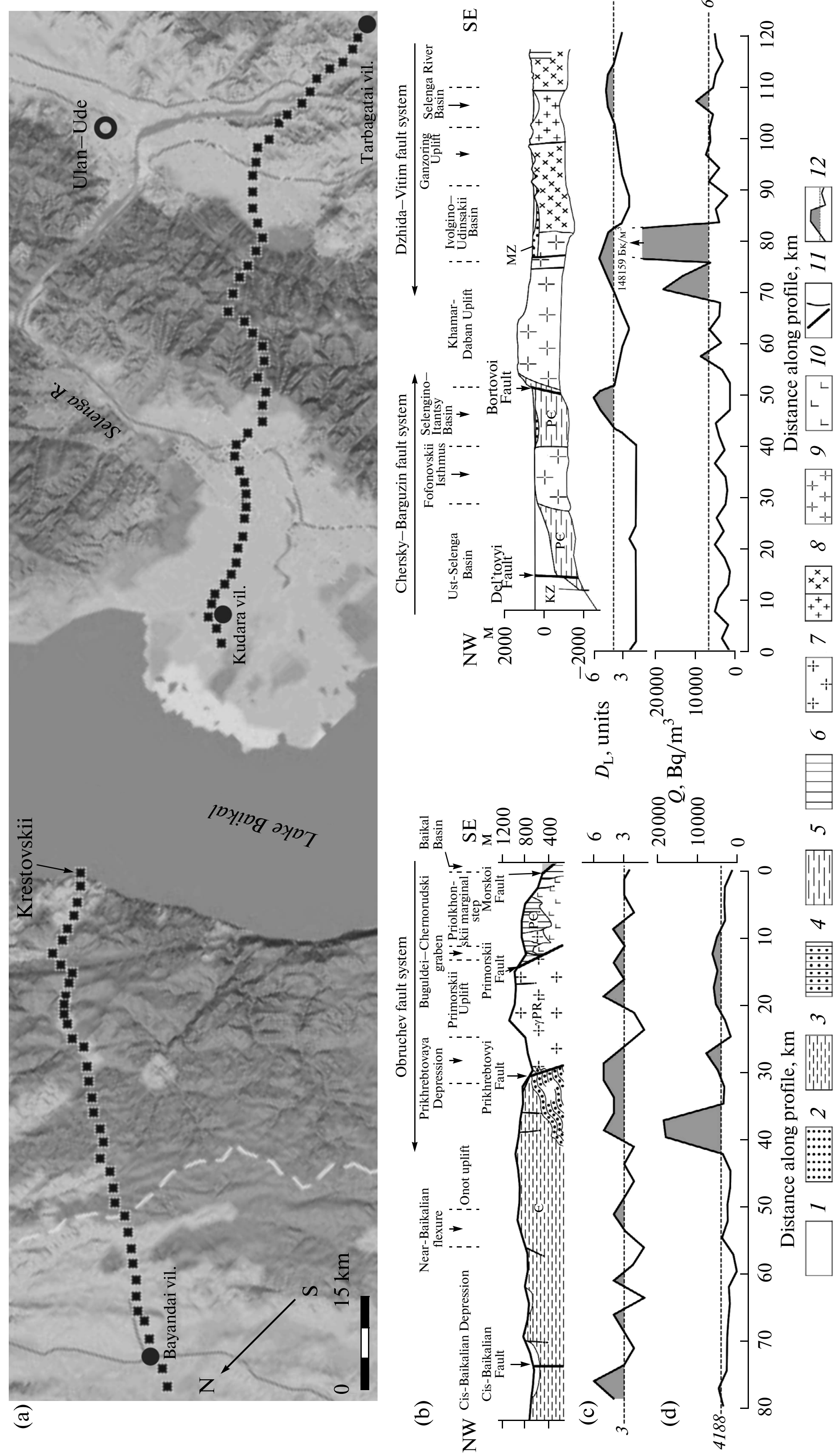
(a)
Krestovskii
Lake Baikal
Selenga R.
Ulan-Ude
Kudara vil.
Tarbagatai vil.
Bayandai vil.
N
S
0 15 km
(b)
NW
SE
Cis-Baikalian Depression
Near-Baikalian flexure
Onot uplift
Obruchev fault system
Prikhrebtovaya Depression
Primorskii Uplift
Buguldei–Chernorudski graben
Priolkhon-ski marginal step
Baikal Basin
Cis-Baikalian Fault
Prikhrebtovyi Fault
Primorskii Fault
Morskoi Fault
(c)
(d)
4188
Distance along profile, km
(e)
Chersky–Barguzin fault system
Dzhida–Vitim fault system
Ust-Selenga Basin
Fofonovskii Isthmus
Selengino-Itantsy Basin
Khamar-Daban Uplift
Ivolgino-Udinsakii Basin
Ganzoring Uplift
Selenga River Basin
Del'toyyi Fault
Bortovoi Fault
KZ
MZ
(f)
D_L, units
(g)
Q, Bq/m^3
6830
148159 Бк/м^3
Distance along profile, km
1 2 3 4 5 6 7 8 9 10 11 12

Fig. 2. (a) The general scheme and the results of the structural, geomorphologic, and emanation surveys along the profiles intersecting (b–d) the western and (e–g) eastern shoulders of the Baikal Rift. (a) The layout of the Bayandai–Krestovskii and Kudara–Tarbagatai profiles against the 3D digital elevation model of Central Baikal region; (b, e) the geological cross sections and main morphotectonic elements (the names are indicated on the top) on the (b) Bayandai–Krestovskii and (e) Kudara–Tarbagatai profiles. The cross sections are constructed by A.V. Cheremnykh (Seminsky et al., 2013); (c, f) the variations in the density of the topographic lineaments (D_L) along the (c) Bayandai–Krestovskii and (f) Kudara–Tarbagatai profiles; (d, g) the variations in the radon activity (Q) along the (d) Bayandai–Krestovskii and (g) Kudara–Tarbagatai profiles. *1*, loose sediments represented by clays, loams, sands, etc.; *2–10*, hard rocks of different types and ages; *11*, the main fault and secondary faults; *12*, the anomalous values of Q and D_L (the dashed line shows the average level over the profile).

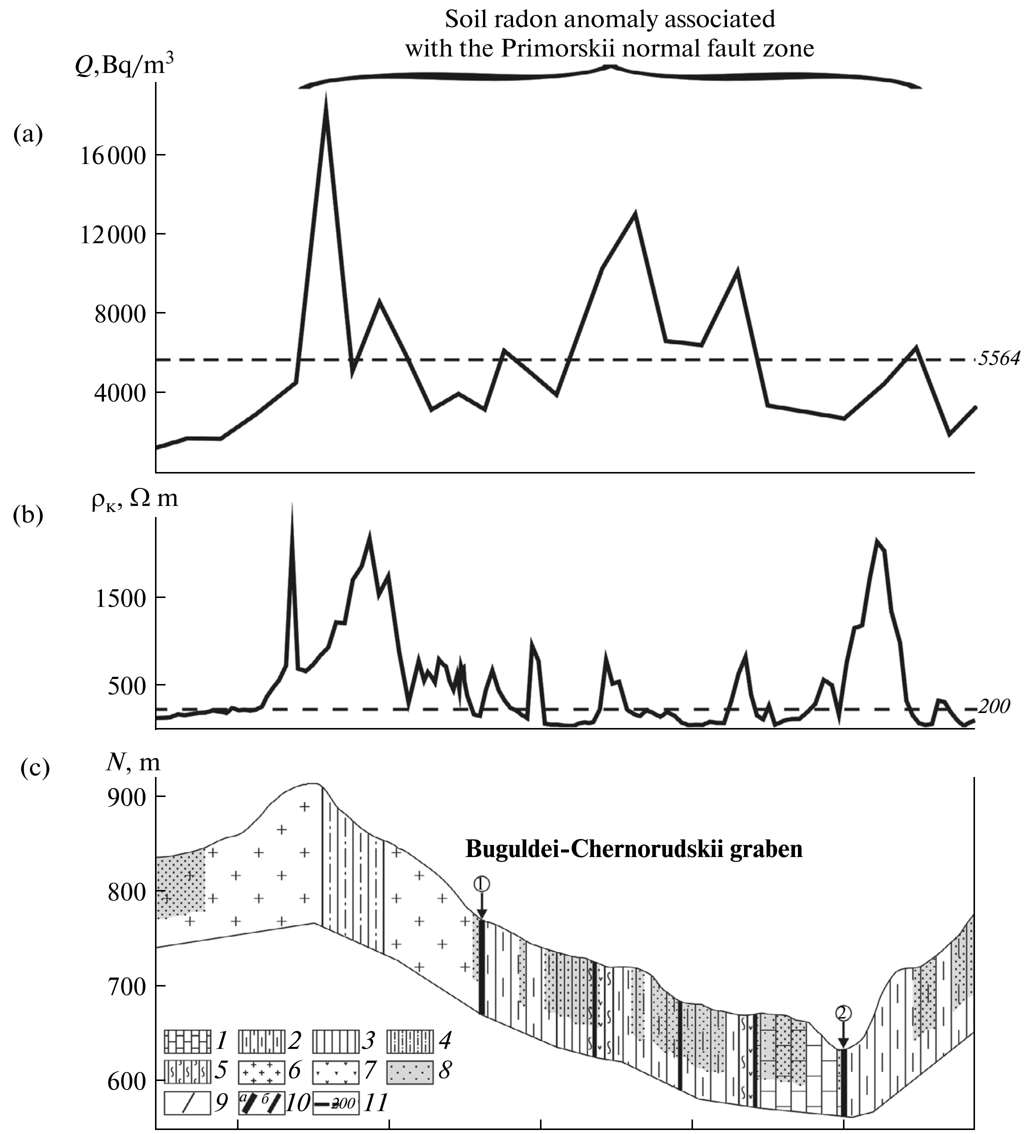

Fig. 3. The results of the geological–geophysical studies along the profile cutting the Primorskaya normal fault zone in the Olkhon region: (a, b) the variations in the (a) radon activity and (b) apparent electrical resistivity according to the data of V.V. Olenchenko (Seminsky et al., 2013); (c) the geological cross section according to the data of Zh.V. Dombrovskaya (1973): *1*, marbled limestone; *2*, two-mica gneiss; *3*, amphibole gneiss; *4*, two-mica gneiss; *5*, migmatite gneiss; *6*, granite and granite-gneiss; *7*, gabbro-diorite; *8*, weathering crust; *9*, rock contact; *10*, (a) the main (*1*. Primorskii normal fault; *2*, Tyrgan–Kuchelgin normal fault) and (b) secondary faults; *11*, the average value of the parameters.

and Tutai normal faults parqallel to it, as well as for the smaller faults exposed across the banks of the Maloe More (Lesser Sea) and Olkhonskie Vorota (Olkhon Gate) straits. In the Central Mongolia, the profile emanation survey with a step of 10–25 m was conducted for 15 faults (Fig. 1b) in the epicentral part of the strong Mogod earthquake, which occurred on January 5, 1967 and had magnitude $M = 7.8$, and in the suburbs of Ulan Bator, where numerous seismic events with $M = 1.0$–2.5 occurred recently during the past few years.

Thus, the emanation survey on the three different spatiotemporal scales provided the possibility to study the distribution of the soil radon across the Baikal region on the levels of the fault systems (e.g., Obruchev system), large fault zones (e.g., Primorskuii fault zine), and separate faults (e.g., Tyrgan-Kuchelgin) having northeastern strikes, i.e., to gain a consistent idea of the radon field associated with the Baikal Rift. Besides, the data for Central Mongolia enabled us to estimate radon activity in the territory with a different landscape and geodynamical conditions than the conditions in the Baikal region.

THE METHODS OF DATA ACQUISITION AND PROCESSING

The profiles of the emanation survey intersect the fault zones across their strikes at the places where the key features of their structures (primarily, the positions of their fault planes) are clearly detectable from the structural and geomorphological observations. The state geological maps with a scale of 1 : 200 000 and the published data served as the basis for constructing the structural cross sections through the large fault systems and fault zones (Figs. 2b and 2e). In order to roughly estimate the permeability of the rock masses along the large profiles, we analyzed the digital elevation models and identified the lineaments (linear or gently bent scarps, flattened segments of the valleys and linear erosional forms), which typically reflect the positions of the active faults in the studied territory (Fig. 1). The structural cross sections through relatively small faults in the Olkhon region (Fig. 4d) rely on the data provided by the studies in the natural outcrops located as close as possible to the emanation profiles (Fig. 4a). The width of the fault zone was estimated from the data on fracture density per square km (D) measured with a step of 2.5–5 m along the structural cross section (Fig. 4c). The graphs of the variations in the activity of soil radon (Fig. 4b) were constructed based on the results of emanation measurements conducted by two methods. The emanation survey in the Baikal region was conducted with the use of the RRA-01M-03 radon radiometer (*Metodika...*, 2004), and the measurements in Mongolia, with the Kamera-01 instruments. The main features of these complexes and their application are briefly described below.

The RRA-01M-03 radiometer has a sensitivity of at least 1.4×10^{-4} c^{-1} Bq^{-1} m^3 and 30% threshold of the admissible relative error. The standard measurement protocol of this device was adjusted to the landscape and weather conditions of East Siberia (Bobrov, 2008), which allowed us to mitigate the influence of air pressure, temperature and air humidity on the estimates of radon activity due to the optimally selected mode of measurements and the depth of sampling. The measurements were conducted from 10 a.m. to 8 p.m. in dry weather conditions. The air samples were taken from a depth of 0.5 m, where the effects of the atmospheric air on Q are significantly reduced. Besides, a point was sampled twice if a sharp change in the air pressure, temperature, or air humidity, whose values were recorded simultaneously with the measurements of Q, occurred during the measurement. For each measurement, a cylindrical hole with a diameter of 2.5 cm was cut in the ground and then hermetically sealed for 30 min. During this time, the radon concentration within the hole and in the soil air was equilibrated. Then, the air sample was pumped into the radiometer and the parameter Q was measured. After each measurement, the system was bled from the air sample by pumping the atmospheric air through the chamber. Each measurement cycle took at most 40 min.

The Kamera-01 system includes the detection block (BDB-13), adsorption cartridges with activated charcoal (adsorbers), and a notebook with the Radon software installed. For determining the values of Q, the cartridge was placed into the ground at the measurement point. The hole with a depth of 5–10 cm with the adsorber inside was covered with a lid in order to protect the charcoal from overdamping and prevent radon escaping into the atmosphere. After two days, the adsorber was retrieved from the ground and the radon-saturated charcoal from the cartridge was placed for testing into the BDB-13 detector connected to the notebook. The results of the measurements of Q, together with a series of additional parameters (the mass of the adsorber before and after the exposure, the times of placement and retrieval, etc.), were used for

Fig. 4. The results of the structural, geomorphological, and emanation studies of the fault zone at Cape Ontkhoi on the Olkhon region: (a) The scheme of isohypses with the profiles of radon emanation survey; (b) the variations in radon activity along profiles 1 and 2; (c) the variations in fracture density per square meter of bedrock outcrop; (d) the structural cross section: *1*, isohypses; *2*, the positions of the (*1*) main and (*2*) secondary faults in the graphs and on the scheme a; *3* the lines of the structural section; *4*, measurement points of radon activity; *5* and *6*, the zones of tectonites near the (*5*) secondary and (*6*) main faults; *7*, the segments of the massif cut by large fractures; *8*, gneisses; *9*, granites–gneisses; *10*, ancient mylonites; *11*, anomalous values of the parameters (the dashed line shows the average level).

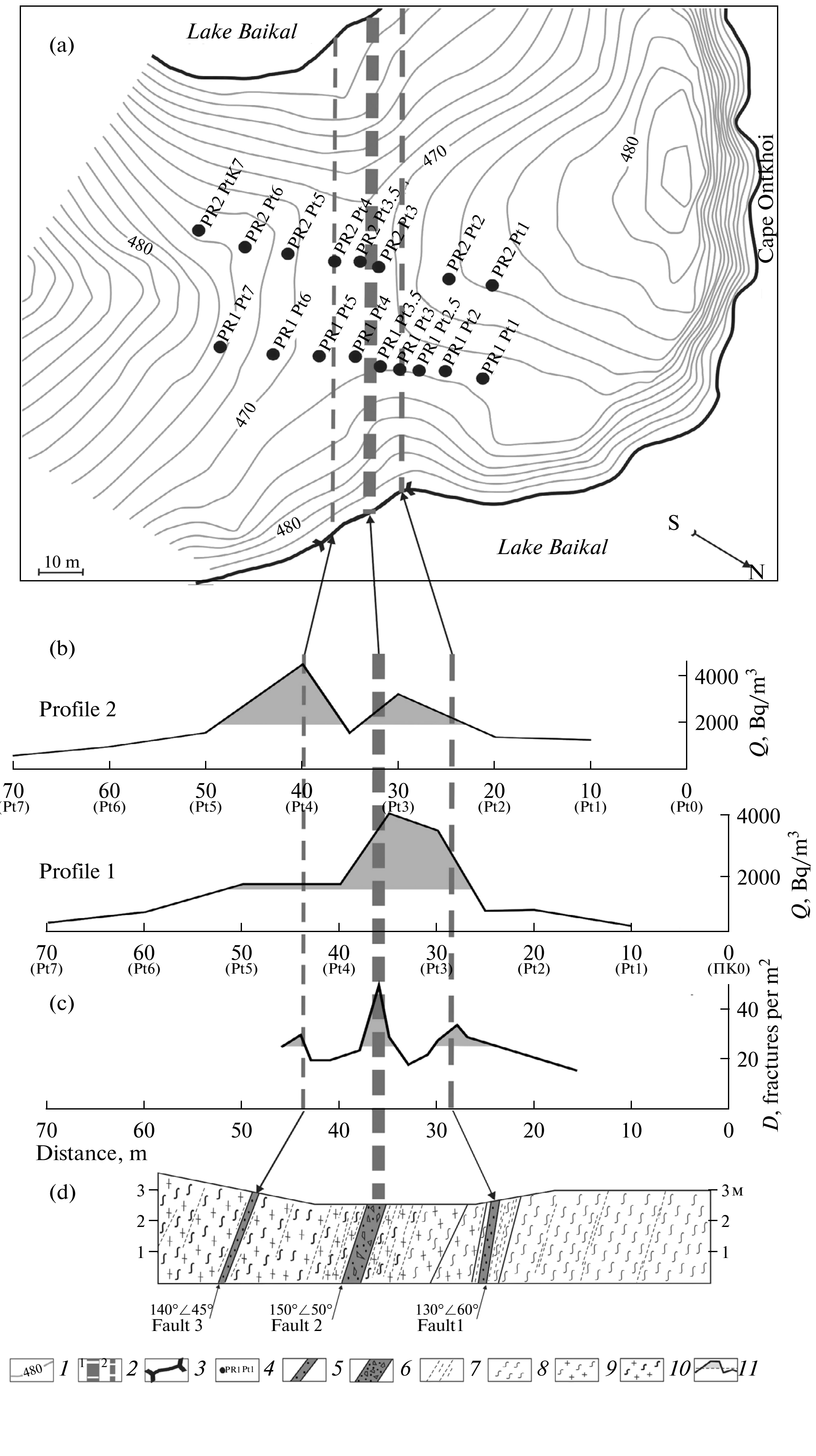
(a)
Lake Baikal
Cape Ontkhoi
470
480
PR2 PtK7
PR2 Pt6
PR2 Pt5
PR2 Pt4
PR2 Pt3.5
PR2 Pt3
PR2 Pt2
PR2 Pt1
PR1 Pt7
PR1 Pt6
PR1 Pt5
PR1 Pt4
PR1 Pt3.5
PR1 Pt3
PR1 Pt2.5
PR1 Pt2
PR1 Pt1
10 m
S
N
(b)
Profile 2
Profile 1
Q, Bq/m³
4000
2000
70 (Pt7) 60 (Pt6) 50 (Pt5) 40 (Pt4) 30 (Pt3) 20 (Pt2) 10 (Pt1) 0 (Pt0)
70 (Pt7) 60 (Pt6) 50 (Pt5) 40 (Pt4) 30 (Pt3) 20 (Pt2) 10 (Pt1) 0 (ПК0)
(c)
D, fractures per m²
40
20
Distance, m
(d)
3 м
140°∠45° Fault 3
150°∠50° Fault 2
130°∠60° Fault1
480 1
2
3
PR1 Pt1 4
5
6
7
8
9
10
11

Table 1. The parameters of the fault zones in the Baikal region estimated from the data of structural and emanation studies

Site	Fault	Width of the zone, m		Q_{max}, Bq/m^3	Q_{min}, Bq/m^3	K_Q
		according to anomaly in H_D	according to anomaly in H_Q			
Kurkut-1	1-1	7	20	2037	746	2.7
Kurkut-1	1-2	5	20	2323	677	3.4
Kurkut-1	1-3	35	40	2651	444	6
Kurkut-2	2-1	25	45	2852	661	4.3
Kurkut-2	2-2	53	60	9921	955	10.4
Kurkut-2	2-3		10	3354	820	4.1
Kuchelga	3		30	19171	3730	5.1
MRS-4	4	30	35	3495	166	21
MRS-5	5-1		12	4452	1698	2.6
MRS-5	5-2	5	10	2865	1595	1.8
Ontkhoi	6	23	24	4752	759	6.3
Sarma	7		30	21118	1846	11.4
Shear-1	8-1		10	13522	3697	3.7
Shear-1	8-2		28	20000	4222	4.7
Tomota	9		75	8048	1148	7
Ulirba	10-1	7.5	8	1214	330	3.7
Ulirba	10-2	20	16	1432	305	4.7

The data on radon activity in the soil air are obtained with the use of the RRA-01M-03 radiometer. Q_{max} is the maximal value of the radon activity in the fault zone; Q_{min} is the minimal value of the radon activity within the wings of the fault; H_D is the width of the fault zone corresponding to the length of the segment of the anomalous fracture density; H_Q is the width of the fault zone corresponding to the length of the segment of the anomalous values of the radon activity; and K_Q is the radon activity index.

processing by the Radon software. This yielded the absolute values of Q at the measurement point averaged over two days. The sensitivity of the Kamera-01 complex with the BNDB-13 beta detection block ranges within 0.27 ± 0.03 Bq^{-1} s^{-1} and the admissible relative error lies within ±30%.

The estimates of the radon activity provided by the different instruments at the same measurement point differ in magnitude. This, however, is not an obstacle for the qualitative analysis of the shapes of the near-fault radon anomalies. For the quantitative comparison of the faults in terms of radon activity, we applied the relative parameter $K_Q = Q_{max}/Q_{min}$, where Q_{max} is the maximal value of Q on the profile (the amplitude of the anomaly) and Q_{min} is the minimal value of Q in the rocks outside the fault zone. For the parameter Q_{min}, we used either the mean of two values determined on the different wings of the fault or one value if it was only possible to capture a part of the fault zone by the survey. The second situation was characteristic of the objects in Mongolia where the detailed structure of the emanation anomaly was studied in the vicinity of the main fault plane forming a prominent scarp in the topography (Fig. 5).

The width of the permeable zone associated with each fault object was determined by the size of the area with the anomalous values of fracture density D if the analysis was based on the structural data (H_D), or by the anomalous area of the Q parameter if the radon data were used (H_Q). The values were treated as anomalous (i.e., characterizing strongly damaged substrate of the fault zone) if they were larger than the average value over a given profile (Q_{mean}). When selecting the threshold distinguishing the background values from

Fig. 5. The results of the radon studies for the zone of the Khustai fault in Central Mongolia: (a) the space image of the segment where the fault plane of the fault zone is expressed by the scarp in the topography; (b) the variations in the activity of soil radon along seven profiles crossing the fault zone; *1*, the position of the fault and its code; *2*, the graph of the variations in Q; *3*, the position of the fault in the graphs; *4*, the level and values of the arithmetic means for the activity of soil radon measured on the profile; *5*, the values of Q for the main maximum in the near-fault anomaly and the minimal value(s) outside it; *6*, the number and place of taking the sample in which the uranium content was estimated; *7*, the segments of the profile with the anomalous values of Q; *8*, the anomalies of the soil radon associated with the fault; *9*, the implied boundary of the soil radon anomaly associated with the fault.

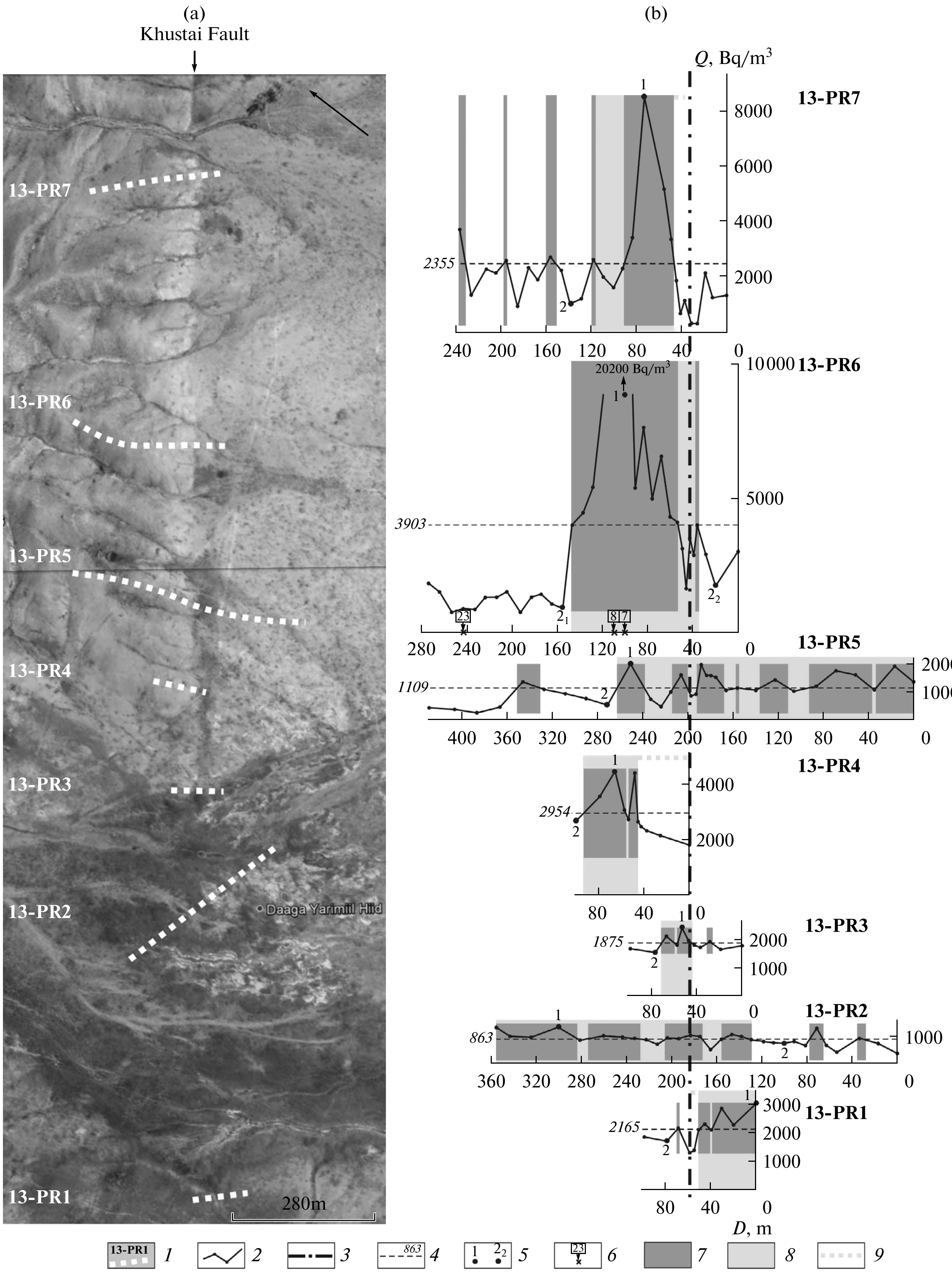
(a)
Khustai Fault
13-PR7
13-PR6
13-PR5
13-PR4
13-PR3
13-PR2
13-PR1
Daaga Yarimiil Hiid
280m
(b)
Q, Bq/m3
D, m
2355
3903
1109
2954
1875
863
2165
20200 Bq/m3
1
2
3
4
5
6
7
8
9

Table 2. The parameters of the fault zones in Central Mongolia based on the data emanation survey

Site	Profile	Name of fault	Q_{max}, Bq/m^3	Q_{min}, Bq/m^3	K_Q	H_Q, m	Position of the fault in radon anomaly
1	13-PR1	Khustai	3110	1770	1.8	>70	min
	13-PR2	Khustai	1310	727	1.8	>230	max
	13-PR3	Khustai	2440	1560	1.6	>30	
	13-PR4	Khustai	4530	2710	1.7	>50	min
	13-PR5	Khustai	1970	523	3.8	>270	min
	13-PR6	Khustai	20200	1168	17.3	>100	max
	13-PR7	Khustai	8460	1010	8.4	>75	min
	2-PR1	SZ-NR	1740	856	2.0	>120	min
	7-PR1	Meridian-NR	4280	1010	4.2	165	min
2	14-PR1	Khustai-VSV	2110	1390	1.5	>55	min
	15-PR1	Khustai-Sh	5460	2195	2.5	105	
3	3-PR1	Emelet-EP	1350	292	4.6	>190	min
	3-PR2	Emelet-EP	1800	400	4.5	>100	min
	3-PR3	Emelet-EP	2930	1490	2.0	45	min
	5-PR1	SSZ-EP	2180	750	2.9	55	min
	6-PR1	M-EP	1820	690	2.6	25	min
	9-PR1	VSV-EP	1550	849	1.8	>30	min
	9-PR2	VSV-EP	1500	594	2.5	>20	
	10-PR1	SV-EP	2020	839	2.4	30	max
	10-PR2	SV-EP	3010	1270	2.4	20	
4	11-PR1	Gundzhin	6560	1371	4.8	80	
5	4-PR1	Kholyiin	4970	347	14.3	390	min
6	12-PR1	Avdar	5740	1470	3.9	300	min
	12-PR2	Avdar	2930	800	3.7	170	
7	8-PR1	Mogod	2380	370	6.4	115	max
	8-PR2	Mogod	1430	787	1.8	>60	
8	1-PR1	Tulet	1160	264	4.4	>110	max
	1-PR2	Tulet	798	575	1.4	>40	max

The measurements of the radon activity in the soil air were carried out with the use of the Kamera-01 instruments. The designations are the same as in Table 1.

the anomalous values, we intentionally rejected the approach applied in the previous studies of our colleagues, who specified this threshold as the arithmetic mean plus the root mean square deviation (RMSD) (King et al., 1993; Walia et al., 2008) or plus half the RMSD (Tansi et sl., 2005). The detailed analysis of some outcrops showed that with their approach, some large faults with slickenlines and splay fractures can fall beyond the fault zone. Even with the use of the criterion of the arithmetic mean, the anomalous values typically occurred on two or three spatially close segments of the profile. If the width of these segments was larger than the length of the intermediate segments with $Q < Q_{mean}$, the total size of the fault zone was determined by the outer boundaries of the extreme segments (Fig. 4b, profile 2; Fig. 5).

Below, the results of the profile radon emanation survey are separately described for the three scales of studies. The emphasis is placed on the analysis of the radon anomalies associated with the elements of each rank of the disjunctive structures. The parameters for the faults that have been explored in finer detail and constitute the majority of the studied objects are presented in Tables 1 and 2.

RESULTS

The Bayandai–Krestovskii and Kudara–Tarabagatai Profiles

The studies on these profiles were aimed at estimating the size and delineating the configuration of the radon emanation anomalies associated with the fault systems that are located within the shoulders of the Baikal Rift.

The distribution of radon concentrations in soils along the Bayandai–Krestovskii profile is highly nonuniform (Fig. 2d). Except for the relatively small Q-anomaly confined to the axis of the Cis-Baikalian depression, all the other anomalies are clustered in the southeastern part of the profile. By their locations and shapes, they correspond to the anomalies in the density of the topographic lineaments and the areas where the faults approach closer to each other, as shown by the structural cross section in Figs. 2b and 2c. The southeasternmost segment (8–21 km on the profile) is clearly associated with the Primorskii normal fault. The secondary faults cut the rocks of the Buguldei–Chernorudskaya depression and the northwestern slopes of the Primorskii uplift, which is reflected in the complicated shape of the anomalies in the Q- and D_L parameters containing two and three peaks, respectively. The southeast's second segment (26–42 km on the profile) manifests itself in the single anomaly of the lineament density with two peaks, each corresponding to a separate Q anomaly. The bimodal structure of this segment is determined by the presence of the Prikhrebtovyi normal fault and the corresponding depression of the same name, as well as by the existence of the fault zone in its rear part, which splits the southeastern slope of the Onot uplift. The structural and geomorphological situation similar to that on the two segments discussed above is also characteristic of the zone controlled by the Morskoi fault. However, a major part of this fault is hidden under the waters of Lake Baikal, which made it impossible to conduct a full-scale study and obtain the expected pattern of distribution of the Q- and D_L parameters.

Thus, the distribution of the soil radon anomalies in the southeastern part of the Bayandai–Krestovskii profile agrees with the topographical features and layout of the faults, which reflect the structure of the Obruchev crustal extension system (Figs. 1a and 2b). Since this fault system relates to the Baikal rift shoulder, it is reasonable to draw the western boundary of the associated radon anomaly at the 42 km mark on the studied profile. This is about 10 km farther to the west of the boundary than is normally assumed for the Baikal Rift (*Karta*..., 1979). The fault-related nature of the emanation anomaly is responsible for its intermittent character with alternating segments of high and low concentrations of soil radon, which have commensurate sizes (Fig. 2d). The minima in Q correspond to the blocks, and the positive anomalies mark the fault zones with the main ruptures of the Prikhrebtovyi, Primorskii, and other large normal faults, which determine the crustal extension in the NW–SE direction.

The variations in the radon activity along the Kudara–Tarbagatai profile are largely similar to those described above for the western slopes of the Baikal Rift (Fig. 2g). However, in this case, distinct correlation between the Q- and D_L anomalies and their association with the negative topographic features are only characteristic for the southeastern part of the profile, where it crosses the Dzhida–Vitim fault system (Figs. 2e and 2f). The anomalous segments are observed in the intervals of 68–83 and 97–110 km along the profile and are caused by the presence of the fault zones composing the system, which are confined to the southeastern slope of the Khamar Daban Ridge and Selenga river basin, respectively. The northwestern part of the profile intersects the Chersky–Barguzin system of crustal extension, which, due to its closeness to the axial part of the rift, accommodates intense displacements along the Bortovoi and, particularly, Deltovyi faults. These displacements result in high seismicity (Suvorov and Tubaniv, 2008) and general subsidence, which captures the area of the lower reaches of the Selenga River and is covered with a thick layer of the Late Cenozoic deposits (Fig. 2e). As a consequence, the anomalies in the concentration of soil radon are absent since gas migration is strongly impeded in the finely dispersed sediments (Al-Bataina et al., 2005; Richon et al., 2010).

Thus, the results of the emanation survey support the reconstructions presented in the previous papers (Levi, 1980; Popov, 1989; Sun Yunshen et al., 1996; Gol'din et al., 2006; San'kov et al., 2009; Seminsky and Radziminovich, 2011, etc.), according to which the Vitim fault zone on the considered segment falls within the limits of the Baikal Rift. The emanation data on the long transects suggest that the near-rift radon anomaly in the Central Baikal region has a width of about 170 km. It comprises separate anomalies, which structurally represent the zones of the large normal faults—the components of the fault systems that turned out to be most permeable for gases in the conditions of crustal extension associated with rifting. A characteristic feature of the cross-fault section of the Baikal anomaly is the confinement of the highest radon concentrations to the marginal areas (Prikhretovyi, Dzhida-Vitim), whereas in the central part of the territory, separate near-fault anomalies are less intense or even absent due to the presence of the layer of low-permeable deposits of the Ust'-Selenga depression and, probably, the sediments of the Baikal Basin.

The Segment of the Bayandai–Krestovskii Profile (11.5 to 16.5 km)

The emanation study was focused on the Primorskaya fault zone, which is part of the Obruchev system of crustal extension and distinguished by the segments of anomalous values of Q in the detailed survey (Fig. 2d). According to the previous data (Dombrovskaya, 1973), the Buguldei–Chernorudskii graben, which represents the studied structure on the profile, comprises the Primorskii and Tyrgan–Kuchelogin normal faults within its slopes and a series of secondary subparallel dislocations in its central part

(Fig. 3c). The rocks composing the graben are weakened due to weathering and dislocation by a dense network of the faults and fractures, whose density was impossible to estimate because of the poorly exposed rocks. The degree of disintegration of the massif was estimated from the data of electrical prospecting (Fig. 3b). The gray segments of the profile (Fig. 3c) reflect highly disintegrated rocks with the apparent resistivity ρ_a of at most 200 Ω m. These values correspond to the high percentage of clay particles formed by the weathering of the intrusive and metamorphic rocks (Palacky, 1989) widespread in the region.

The nonuniform disintegration of the rocks composing the graben produces significant variations in the activity of soil radon (Fig. 3a). The anomaly associated with the Primorskaya normal-fault zone has a width of 4100 m and stretches for 1200 and 500 m on the either side of the bordering faults. It covers five closely located segments of the profile with $Q > Q_{mean}$; however, these segments correspond to the blocks confined between the faults but not to the faults (Fig. 3c). The high permeability of the blocks and segments located on the outer side of the bordering faults are accounted for by the existence of the network of open fractures, which are formed in the massif due to active movements in the Prirazlomnaya fault zone. In contrast, the separate faults, together with the splay fractures branching from them, are lowly permeable and thus unfavorable for the migration of gases due to the presence of the fine dispersed filler material in them. By analogy with the results of the previous studies, it could be the clay gouge and/or the products of rock weathering (Bali et al., 1991; King et al., 1993; Seminsky and Bobrov, 2009a). Due to this, variations in Q and ρ_a along the considered profile are similar (Figs. 3a and 3b).

Thus, the anomaly in the radon concentration in the soil above the Primorskaya fault zone has a complex structure. This conclusion is supported by the results of the electrical profiling and emanation survey on the profile located 3 km southwest of the long transect described above. Here, the internal, weakly dislocated blocks of the graben have lower Q than the fault zones, each marked with the anomaly having a narrow minimum in the central part corresponding to the main fault. Therefore, the gas emanation in this case is only impeded by the clay gouge, while the weathering processes are far less intense than on the main transect where their finely dispersed products strongly obscure the manifestations of the fracture structure of the Primorskaya fault zone in the emanation field.

The Detailed Profiles in the Baikal Region and Central Mongolia

The features of the soil radon anomalies revealed by the studies on the rift disjunctives in the Olkhon region are illustrated below by the example of the zone of a small fault on Cape Ontkhoi in the southwestern part of the Maloe More Strait (Figs. 1a and 4). For the territory of Central Mongolia, we analyze the main fault of the Khustai fault zone approaching Ulan Bator in the southeast (Figs. 1b and 5). These tectonic dislocations, just as the other faults studied on this scale of survey, are associated with the anomalous values of the activity of soil radon, which, according to the relationships previously derived for the Olkhon region (Seminsky and Bobrov, 2009b), coincide with or are slightly larger than the segments with anomalous fracture density. At the same time, the shapes, sizes, and intensities of radon anomalies are very diverse. We note the following most common features.

In the simplest cases, the cross section of the segment of anomalous Q has a single maximum with a gradual or stepwise decrease in the soil radon concentration towards the periphery (Fig. 4b, profile 1). However, in most of the studied situations, the radon anomaly is more complex and, as a rule, intermittent, which is associated with the heterogeneous structure of the fault zone. The most prominent fractures within this zone produce local extrema in Q, which are either positive when the fault is filled with permeable fracture breccia (Fig. 4b, profile 2) or negative when the tectonites have undergone intense weathering or exist in the form of clay gouge (Fig. 5b). The dedicated analysis of the positions of the main faults against the anomaly in the fault zones in Mongolia shows (Table 2, Fig. 5b) that in most cases (15), the fault is located in the area of the maximum in Q; in six fault zones it falls in the minimum in Q, and in seven cases it occurs within the intermediate segments (in the most cases, this is the marginal part of the anomaly). As a consequence, the cross sections of the anomalies are typically asymmetric.

The variability of the radon field is also clearly expressed along the strike of the fault, as illustrated by the both examples (Figs. 4 and 5) but is most striking in the Khustai fault zone, which is intersected by a few closely located profiles. The shape of the radon anomaly and the position of its axis with Q_{max} is different in the southwestern (Fig. 5b, profile 13-PR1) and the southeastern (Fig. 5b, profiles 13-PR3...13-PR7) segments of the Khustai fault separated by a transverse valley of fault origin. The confinement of the maximal values of Q to the northwestern wing of the fault, which is observed on four northeastern profiles, is the most persistent spatial feature of the studied distribution. Here, the axis of the radon anomaly is distinctly traced at approximately equal distance (55 m) from the main fault. Southwest of the 13-PR4 profile, the shape of the distribution of radon concentration changes significantly. One of the simple explanations of this feature is probably associated with the position of the profiles in the marginal (13-PR1 and 13-PR3) and central (13-PR2) parts of the river basin (Fig. 5a), where the Quaternary deposits overlay the Khustai fault and obscure the manifestation of the near-fault radon anomaly.

The quantitative characteristics of emanation anomalies—the width (H_Q), intensity (Q_{max}), and radon activity factor K_Q—differ between the disjunctives of the studied group (Tables 1 and 2) and along the individual fault zones, which is most clearly illustrated in Fig. 5b. The width of the radon anomaly associated with the Khustoi fault significantly varies along the strike, where its estimation is complicated by the uncertain geometrical relationship between this anomaly and the main fault (profiles 13-PR1, 13-PR4, and 13-PR7), the presence of feathering fractures (13-PR5), or blanking of the zone by the layer of relatively young sediments (13-PR2). The intensity and gradients of this anomaly estimated in its different cross sections differ by an order of magnitude and more (by a factor of ~15 for Q_{max} and by a factor of ~10 for K_Q). The large span of these quantities is commensurate with the differences in the intensity and contrast between the anomalies established at the present stage of studies for different faults in Mongolia and the Olkhon region (tables 1 and 2). We note that profile 13-PR5, where the radon intensity is one of the lowest (1970 Bq/m^3), runs very close (at ~300 m) to the transect of the fault by the 13-PR6 profile, where Q_{max} (20 200 Bq/m^3) is not only the highest among the values known for the Khustai fault but also across the Central Mongolia overall. The geochemical factor has no bearing on the formation of the discussed anomaly, as suggested by the analysis of the rock samples by the method of inductively coupled plasma mass spectroscopy carried out at the laboratory of geochronology and isotopy of the Institute of the Earth Crust of the Siberian Branch of the Russian Academy of Sciences. This analysis established a small and nearly uniform uranium concentration (1.53–1.73 μg/g) in the rocks above which the soils have high (points 7 and 8) and low (point 23) radon concentrations (Fig. 5b, profile 13-PR6).

Due to the extremely nonuniform radon distribution above the faults in the Olkhon region and Central Mongolia, the adequate estimation of the parameters of emanation anomalies is challenging. In the example illustrated by Figs. 4 and 5 it can be seen that the missing interval of high Q near the main fault, incomplete capturing of the near-fault anomaly, or the study of emanation anomalies on as few as one or two profiles may produce significant errors in estimating the radon activity of the fault zone. This raises more demanding requirements on the procedure of the emanation survey and interpretation of the results.

DISCUSSION

The interpretation of the results of the profile emanation survey over two different-type regions of the Mongolia–Baikal seismic belt indicates the critical role of the fault dislocations of the Earth's crust for the spatial distribution of soil radon. In the Baikal region, where the studies involved the fault zones of all the main hierarchical levels, this is most distinctly reflected in the structure of the emanation anomaly associated with the evolution of the Baikal Rift (Fig. 1a). Within the rift, anomalous radon concentrations mark the Obruchev and Dzhida–Vitim systems of the crustal extension located on the western shoulder of the rift and along the periphery of the eastern shoulder (Fig. 2). Within these systems there is a series of closely located segments coinciding with the large fault zones (Primorakaya, Prikhrebtovaya, Uda–Vitim, etc.), where the radon activity is above average. The more detailed studies of radon anomalies in the Primorskaya fault zone of the Olkhon region (Figs. 3 and 4) have demonstrated, in turn, the consistent correlation between gas emanation and the structure and density of the fractures near the faults of the regional and local ranks.

Considering the general consistence of the structural profile of the Baikal Rift, it is reasonable to expect that the described regularities of spatial distribution of soil radon are also characteristic of the territories located in the northeast and southwest of the Central Baikal region, which has been studied in sufficient detail. Thus, it can be hypothesized that the structural-geodynamic factor controls the character of the spatiotemporal distribution of radon anomalies in the Baikal region overall. This factor also affects the intensity of the anomalies, since the concentrations of soil radon up to a few hundred thousand Bq/m^3, which were revealed by our studies on the eastern shoulder of the Baikal Rift (Fig. 2g) and by the previous studies (Koval' et al., 2006) in the other areas in the Baikal region, are confined to the zones of the large faults. The special studies of the compositions of the rocks in the zone controlled by the Khustai fault have shown that the formation of the most intense radon anomaly known for Central Mongolia is not related to geochemical factors. At the same time, the radio activity of the tectonites and unconcolidated fault filler material within the anomalous segments of the Baikal region and Mongolia have not been studied systematically and on a mass basis. This constrains the conclusions presented below to be only applicable for the standard radioactive situations when the uranium concentration in the rocks is not anomalous.

Despite the type and rank distinctions between the fault zones, the distribution of the radon activity within these zones has certain common features. The key similarity between the radon distributions in these zones is their spatial heterogeneity caused by the nonuniform permeability of the fault zone for gases. In this sense, the soil radon anomalies revealed at the intersections of the faults are classified into continuous and intermittent. In the first case, the heterogeneous distribution of parameter Q is expressed by the decrease of Q from the near-axial maximum towards the lower values on the margins of the fault

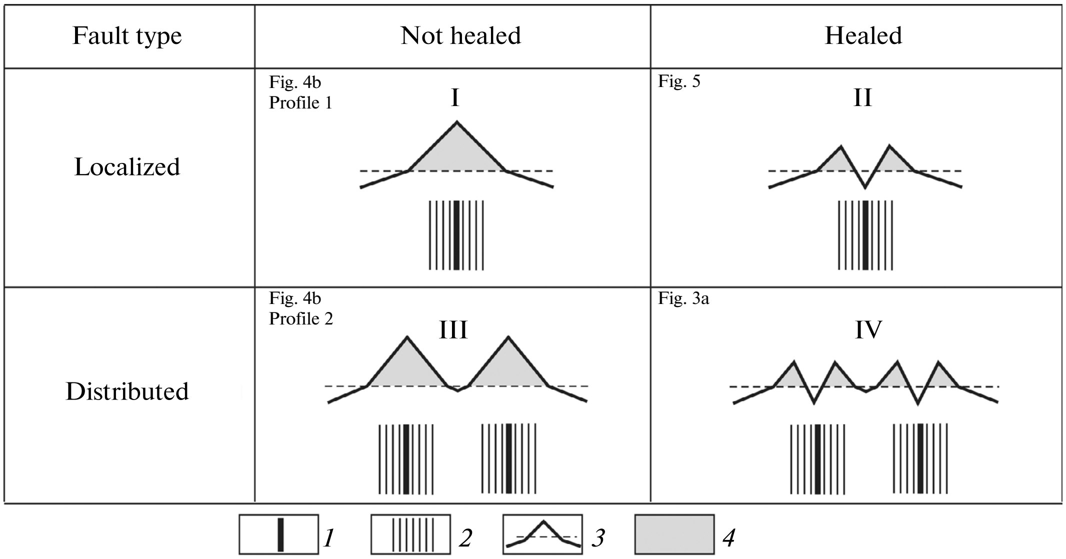

Fig. 6. Manifestations of the four structural situations determined by the type of the fault (localized or distributed) and/or the presence of the filler in the fault (healed or not healed) in the distributions of the radon activity: *1*, the zone of the main fault; *2*, the zone of the associated fracturing; *3*, the cross-fault variation in the activity of soil radon (the dashed line shows the average value); *4*, the field of the anomalous values of the parameter.

zone. These anomalies are characteristic of a few fault zones in the Baikal region and Mongolia (e.g., Fig. 4b, profile 1) and some faults in the other regions (Ioannides et al., 2003; Moussa and El Arabi, 2003; Font et al., 2008; Spivak, 2010).

In the second case, heterogeneity manifests itself by the patchwork structure of the anomaly, which contains the segments where the soil radon concentrations do not exceed their average level. Most objects studied in the Baikal region and Mongolia have anomalies of this type, although the factors responsible for the generation of the segments with low Q are different. For the faults studied here (e.g., Fig. 5) and the faults in California (King et al., 1993; Erzinger, 2008), the existence of the internal segments with low Q is associated with the filling of the fault by the clay gouge or fine dispersed products of weathering, which are impermeable for gases. These faults, just as the disjunctive structures producing continuous anomalies, belong to the localized type of faults: the degree of permeability of the faults and fractures feathering the main fault generally increases from the ambient rocks to the central part. The fault zones of the distributed type are characterized by the presence of a system of secondary fractures with the blocks of relatively intact rocks between them. The low permeability of these blocks determines the intermittent character of the soil radon anomalies above some faults (Fig. 4b, profile 2).

Yet another cause of the intermittency is associated with the influence of the erosion processes, which intensely level up the highly contrasting topography of the fault zones. In combination with weathering, these processes facilitate the formation of basins filled with finely dispersed material that significantly alters the gas permeability of the fault zones. For instance, due to weathering, the internal blocks and the slopes of the Buguldei–Chernorudskii graben have become most permeable for radon (Fig. 3), in contrast to the Primorskii and Tyran–Kuchelgin boundary faults. Due to the filling of the fault-related basins with sediments, radon anomalies can either be absent within these areas or be only present above the boundary faults (Al-Bataina et al., 2005). The Ust-Selenga basin whose sediments act as a screen for radon emanation through the faults of the Chersky–Barguzin system (Figs. 2e–2g) illustrates this situation in the Central Baikal region. It can be hypothesized that the radon anomaly associated with the Baikal Rift overall is bimodal with two maxima in Q confined to the marginal fault systems (Obruchev and Dzhida–Vitim) and the minimum in the central part of the region, where there is a thick layer of Cenozoic sediments (3.5–8 km) hidden by the waters of Lake Baikal.

Thus, the occurrence of the continuous and patchy anomalies is associated with a number of factors resulting in the nonuniform permeability of a fault for gases. The results of our study in the Baikal region complemented with the published data suggest that there are four main situations controlling the pattern of radon anomaly in the cross-fault section (Fig. 6). These situations reflect the combination of the structural pattern of a fault (localized or distributed) and its filling with the finely dispersed material of different origin (healed or not healed). In the cells of the plot, the references are given to the corresponding figures of the present paper that illustrate each situation.

The continuous radon anomaly only arises above a localized permeable fault (I). In the other cases (II–IV), the anomalies are intermittent. A localized fault, whose permeability is strongly damaged, is characterized by the break in anomaly (II). The size of the break is minimal if the fault is filled with the clay gouge and maximal if the permeability of the fault was obstructed by intense weathering or blanketing of a part of the fault zone by fine dispersed sediments. A permeable distributed fault forms an intermittent anomaly if the central, weakly dislocated block is not overlapped by the anomalies from the bordering faults (III). The radon anomaly above the distributed fault with damaged permeability comprises a few segments where the concentration of soil radon is below average (IV).

Figure 6 provides a clear illustration of the uncertainties associated with identifying the boundaries, structural features, and, especially, the activity of the fault zone based on the data of the radon emanation survey. The maxima in the radon activity in the situations of types I and III reflect the traces of the main faults, whereas in the situations of types II and IV they are formed above the peripheral parts of the zone of the accompanying fracturing, and, remarkably, the shapes of the anomalies of the second and third type are generally similar. Clearly, identification of radon anomalies and diagnostics of the fault structure from the data of the emanation survey becomes consistently more difficult in series I–IV. The fault zone may appear in the distribution of Q as not a single entity if the situation of four type is complicated by intense weathering or blanketing of a significant part of the area by fine dispersed material. Besides, it should be taken into account that in the real conditions, the anomalies typically have a complex (combined) type, as shown, e.g., by the neighboring transects of the zone of the Primorskii normal fault. Finally, the fault zones may differ by the number of secondary faults, their parameters (width, dip angle, type of tectonites, etc.) and the degree of filling. All these factors significantly sharpen the heterogeneity of the soil radon anomaly, which in this case comprises a set of maxima and minima of Q with different shapes, widths, and intensities. These anomalies are characteristic of the geodynamically active regions, as is clearly demonstrated by the example of the cross-fault variations of Q in the fault zones of the Olkhon region (Fig. 3).

In light of this, the fact of heterogeneous structure of the soil radon anomalies along the strike of the faults becomes evident. In our studies, this was reflected by the different shapes of the graphs depicting the volumetric radon activity on the profiles that transect the fault at close distances from each other (Figs. 4b and 5). According to the data of areal surveys carried out in different regions of the world (Ciotoli et al., 1999; Moussa and El Arabi, 2003; Tansi et al., 2005; Buttafuoco et al., 2007; Fu et al., 2008; Lombardi and Voltattorni, 2010; Walia et al., 2010), the faults are typically expressed by the chains of maxima in the concentrations of soil radon, between which Q can reach its minimal values. The similar distribution is characteristic of the fracture density in the fault zones of different types and ranks studied in the natural in situ conditions and in the uniform elastoplastic models (Seminsky, 2003).

Thus, the structural complexity of the fracture networks, in combination with the impacts from the erosion processes, produces heterogeneous distribution of the soil radon concentrations along and across the strikes of the fault zones. The basic features of the spatial variations (Fig. 6) indicate that within the poorly exposed territories, the application of the radon survey is only efficient in a limited set of structural situations. The efficiency of this method in delineating the boundaries and revealing the structural features of the fault zones can be increased by measuring and analyzing Q for a possibly larger number of the disjunctive structures in different natural regions.

The experience of our emanation studies in the Baikal region and Mongolia, which differ in landscape, climate, and the geodynamical conditions of the formation of radon anomalies, suggests a series of important recommendations concerning the procedure of the emanation survey, which would be helpful for revealing and estimating these anomalies. This is primarily constructing the long profiles, densifying the measurements in the immediate neighborhood of the main fault, and applying the arithmetic mean as a threshold for identifying the anomalies. For estimating and comparing the radon activity of the faults that belong to different regions, in addition to the normally applied parameters of the intensity ($Q_{\max}$) and width (H_Q) of the anomaly, it is also reasonable to use the relative parameter $K_Q = Q_{\max}/Q_{\min}$, where $Q_{\min}$ is the minimal value of the radon activity immediately outside the limits of the near-fault anomaly.

The quantitative estimates provided by the profile survey on a detailed scale (Tables 1 and 2) show that the values of H_Q, $Q_{\max}$ and K_Q strongly differ among the near-fault anomalies. This is due to the significant variability in the stress state of the rocks in the active fault zones caused by a series of different factors, both external and internal with respect to the solid Earth. As has been shown previously (Seminsky and Bobrov, 2009a; 2013), the parameters of the radon anomalies in the Olkhon region are sensitive to the planetary impacts, which affect the air pressure, and are controlled by the character of the geodynamical activity of the crust. Here, among the parameters of the fault that are derivative from the last factor (the morphogenetic type, rank, and the degree of activity), the strongest impact on radon activity of a tectonic dislocation is caused by the degree of its geodynamical activity.

At the same time, the synthesis of the results provided by the detailed emanation surveys in the Baikal region and Central Mongolia unambiguously demonstrates how misleading the estimates of the geodynamical activity of the fault could be if they are directly tied

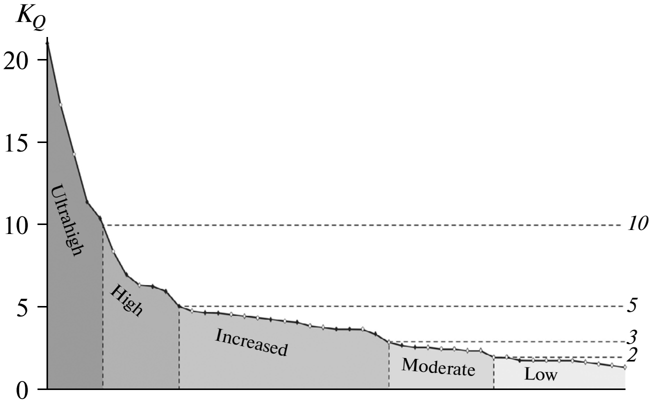

Fig. 7. The graph illustrating the comparison between the near-fault emanation anomalies in terms of radon activity index K_Q. The values of K_Q for the faults of the Baikal region and Mongolia by the black and white dots, respectively, are plotted in the graph in the decreasing order. The areas with different gradations of gray reflect the classification of the studied objects in terms of their radon activity.

to the parameters of the near-fault radon activity. This primarily concerns the estimates based on the absolute value of the intensity of the emanation anomaly Q_{max}, because this quantity depends on factors of the local action: the type of the source of radiation, the physical properties of the ambient rocks, the dynamics of weather conditions, etc. For example (Table 2), according to the value of Q_{max} (2380 Bq/m^3) measured on the shear seismodislocation, the fault that was ruptured by the strongest Mogod earthquake ($M = 7.8$, January 5, 1967) and is characterized by high seismic activity at present, cannot be classified as a disjunctive dislocation with high radon activity. However, this fault becomes such if, for comparison, we apply the relative parameter of radon activity K_Q, which does not depend on the local factors listed above, and use its value that was measured at one of the intersections of this seismodislocation (6.4) and indicates the highly contrasting radon anomaly near the fault.

Thus, it is preferable to estimate the radon activity and, especially, the geodynamic activity in terms of K_Q rather than Q_{max}. Therefore, the data for Mongolia support the conclusion that was previously derived from the study of the Baikal faults. Moreover, it was established (Seminsky and Demberel, 2013) that the values of K_Q obtained for Central Mongolia form certain modes, which made it possible to objectively subdivide the analyzed sample of the structures into five groups. These groups correspond to the ultrahigh ($K_Q > 10$), high ($10 \geq K_Q > 5$), increased ($5 \geq K_Q > 3$), moderate ($3 \geq K_Q > 2$), and low ($K_Q \leq 2$) radon activity (Fig. 7). The addition of the data for the Olkhon region (the black dots) has not changed the general pattern of the distribution, and the estimate for the Primorskii normal fault ($K_Q = 21$) determined near the Sarma seismodislocation has become the maximal estimate in the first group.

According to the described data (Fig. 5b, Table 2), K_Q can vary along the strike of the fault within an order of magnitude and even stronger. For the Khustai fault zone, the tenfold variations in the degree of the contrast of the anomaly occur between profiles 13-PR6 ($K_Q = 17.3$) and 13-PR4 ($K_Q = 1.7$), i.e., within a distance of 500 m, where, according to the geological and geomorphologic data, the radioactivity of the rocks and the thickness of the overlying sediments remain unchanged. Therefore, the formation of the anomaly in this case is controlled by the state of the ruptured structure and the stress filed on the segments of the fault zone, which determine the permeability of the medium for gases in the presence of weathering impacts complicating the situation. This conclusion supports the efficiency of criterion K_Q for determining the relationships between the radon and geodynamical activities of the crustal fault zones, which are important for the further practical applications but are still uncertain. With this approach, for estimating the radon activity of a fault, it is generally reasonable to apply the highest K_Q values of those measured for the separate intersections; and the adequacy of this estimate will depend on the degree of detail of the profile survey.

CONCLUSIONS

The tectonophysical interpretation of the results of emanation survey carried out on three spatial scales on the disjunctive structures of the Mongolia–Baikal seismic belt revealed the common regularities in the pattern of the soil radon anomalies associated with the structures of different spatial sizes: small and large fault zones, fault systems, and, to a certain extent, the Baikal Rift overall. According to the three tasks of this study, these regularities are as follows.

1. In the standard geochemical conditions for uranium, the distribution of soil radon above the fault zones in the Baikal region and Central Mongolia is governed by the structural geodynamical controls. The distribution, direction of action, and intensity of the strain forces control the size, structure, and activity of the fault zone, which, in turn, predetermines the size, shape, and degree of contrast of the soil radon anomaly. For example, the emanation field in the contact zone of the Siberian and Transbaikalian lithospheric blocks is determined by the high permeability of the rocks of the Baikal Rift which is actively developing in the conditions of crustal extension. The cross dimension of the first-order emanation anomaly corresponding to the Baikal Rift in the Central Baikal region is above 170 km, and the radon activity reaches 148 159 Bq/m^3. The internal structure of the anomaly is due to the hierarchy of the fault structures (systems and zones) and the blocks which generate the set of the higher-order anomalies; besides the predominant fracturing, the presence of

the finely dispersed products of the erosion processes and weathering also contributed to (typically, complicated) the formation of these anomalies.

2. The anomalies in the soil radon above the faults are distinguished by spatial heterogeneity, which is associated with the variations in the permeability of the substrate in the fault zone and in the zone of the accompanying fracturing. The cross sections of these anomalies form four basic groups, which are determined by the presence/absence of filler material in a localized/distributed fault. In the simple case of a localized and nonhealed fault, the radon activity gradually increases from the periphery to the main fault. In the most complex case, i.e., in the presence of low permeable blocks and a system of secondary faults with a fine dispersed filler (clay gouge, weathered rocks, clay sediments), the anomaly appears as alternating segments of high and low radon activity. Two intermediate cases give similar (bimodal) anomalies with a central axial minimum and two peripheral maxima. However, in one case the minimum is located above the main fault filed with the clay gouge, while in the other case it occurs above the block between two permeable secondary faults.

3. The degree of radon activity of a fault is reflected in the index K_Q, which is determined from the data of the profile survey as the ratio between the intensity of the near-fault emanation anomaly (Q_{max}) and the minimal radon activity immediately outside the anomaly. Compared to Q_{max}, this relative parameter is less sensitive to weather conditions, the thickness of the overlying sediments, and the radioactivity of the rocks, since it reflects the degree of the contrast of the emanation anomaly near the fault, which is mainly determined by the state of its internal structure and the degree of its geodynamical activity. In the Baikal region and Central Mongolia, the value of K_Q, although varying by a factor of ten, still gravitates to certain levels. This provides the grounds for classifying the faults of the Mongolia–Baikal seismic belt into the groups with low ($K_Q \leq 2$), moderate ($2 < K_Q \leq 3$), increased ($3 < K_Q \leq 5$), high ($5 < K_Q \leq 10$), and ultrahigh ($K_Q > 10$) radon activity.

Our analysis suggests a generally complicated spatial distribution of radon gas above the faults in the studied and probably other natural regions. For particularizing the established regularities, it is required to significantly expand the databank on radon activity for the tectonic dislocations of the Earth's crust. The formation of this databank should rely on a unified approach to radon sampling, data processing, and interpreting the results. One of the possible scenarios of such an approach is described in the present paper.

ACKNOWLEDGMENTS

We are grateful to the members of the laboratory of tectonophysics of the Institute of the Earth's Crust, Siberian Branch of the Russian Academy of Sciences Cand. Sci. (Geol.–Mineral.) A.V. Cheremnykh, Cand. Sci. (Geol.–Mineral.) S.A. Bornyakov, A.S. Cheremnykh, R.M.Zaripov, Yu.P. Burzunova, and E.I.Kogut, member of the Research Center for Astronomy and Geophysics, Academy of Sciences of Mongolia D. Ganzorig, Assoc. Prof. of Irkutsk University for Technology Cand. Sci. (Geol.–Mineral.) M.A. Tugarina, and other specialists for their help in the field measurements and processing the data. We are also grateful to the Head of the laboratory of isotopy and geochronology of the Institute of the Earth's Crust, Siberian Branch of the Russian Academy of Sciences Prof. S.V. Rasskszov and Cand. Sci. (Geol.–Mineral.) T.A. Yasnygina for their help in conducting the inductively coupled plasma mass spectroscopy analyses of the hard rock and the interpretation of the results. The work was supported by the Russian Foundation for Basic Research (project 12-05-00322) and Targeted Federal Program "Academic and Educational Staff for Innovative Russia in 2009–2013" (agreement 14.B37.21.0583).

REFERENCES

Adiya, M., Ankhtsetseg, D., Baasanbat, et al., *One Century of Seismicity in Mongolia (1:2500000 map)*, Research Center of Astronomy and Geophysics, Mongolian Academy of Science and Departement Analyse Surveillance Environnement, CEA-France, Dugarmaa, T. and Schlupp, A., Coordinators, 2003.

Adushkin, V.V., Spivak, A.A., and Kharlamov, V.A., Effects of Lunar–Solar tides in the variations of geophysical fields at the boundary between the Earth's crust and the atmosphere, *Izv., Phys. Solid Earth*, 2012, vol. 48, no. 2, pp. 93–103–26.

Al-Bataina, B.A., Al-Taj, M.M., and Atallah, M.Y., Relation between radon concentrations and morphotectonics of the Dead Sea transform in Wadi Araba, Jordan, *Radiat. Meas.*, 2005, vol. 40, pp. 539–543.

Angelone, M., Gasparini, C., Guerra, M., et al., Fluid geochemistry of the Sardinian rift-Campidano graben (Sardinia, Italy): fault segmentation, seismic quiescence of geochemically "active" faults, and new constraints for selection of CO2 storage sites, *Appl. Geochem.*, 2005, vol. 20, pp. 317–340.

Atallah, M.Y., Al-Bataina, B.A., and Mustafa, H., Radon emanation along the Dead Sea transform (rift) in Jordan, *Environ. Geol.*, 2001, vol. 40, pp. 1440–1446.

Ball, T.K., Cameron, D.G., Colman, T.B., et al., Behaviour of radon in the geological environment: a review, *Quart. J. Eng. Geol. Hydrogeol.*, 1991, vol. 24, pp. 169–182.

Bobrov, A.A., Study of radon activity in the fault zones of the Olhon and Southern Angara regions: techniques and preliminary results, *Izv. Sib. Otd. Sektsii Nauk Zemle RAEN. Geol. Poiski Razved. Rudn. Mestorozhd.*, 2008, vol. 32, no. 6, pp. 124–129.

Buttafuoco, G., Tallarico, A., and Falcone, G., Mapping soil gas radon concentration: a comparative study of geostatistical methods, *Environ. Monit. Assess*, 2007, vol. 131, pp. 135–151.

Chernyago, B.P., Nepomnyashchikh, A.I., and Kalinovskii, G.I., Soil-to-dwelling radion isotope ratio in the

Baikal region, *Rus. Geol. Geophys.*, 2008, vol. 49, no. 12, pp. 971–977.

Chernyago, B.P., Nepomnyashchikh, A.I., and Medvedev, V.I., Current radiation environment in the Central Ecological Zone of the Baikal Natural Territory, *Rus. Geol. Geophyz.*, 2012, vol. 53, no. 9, pp. 926–935.

Cicerone, R.D., Ebel, J.E., and Britton, J., A systematic compilation of earthquake precursors, *Tectonophysics*, 2009, vol. 476, pp. 371–396.

Ciotoli, G., Etiope, G., Guerra, M., et al., The detection of concealed faults in the Ofanto Basin using the correlation between soil-gas fracture surveys, *Tectonophysics*, 1999, vol. 301, pp. 321–332.

Delvaux, D., Moyes, R., Stapel, G., et al., Paleostress reconstruction and geodynamics of the Baikal region, Central Asia. Part II: Cenozoic rifting, *Tectonophysics*, 1997, vol. 282, pp. 1–38.

Dombrovskaya, Zh.V., *Paleogenovaya kora vyvetrivaniya Tsentral'nogo Pribaikal'ya* (The Paleogene Weathering Crust of Central Baikal region), Moscow: Nauka, 1973.

Duddridge, G.A., Grainger, P., and Durrance, E.M., Fault detection using soil gas geochemistry, *Quart. J. Eng. Geol. Hydrogeol.*, 1991, vol. 24, pp. 427–435.

Font, L., Baixeras, C., Moreno, V., et al., Soil radon levels across the Amer fault, *Radiat. Meas.*, 2008, vol. 43, pp. S319–S323.

Fu, C.-C., Yang, T.F., Du, J., et al., Variations of helium and radon concentrations in soil gases from an active fault zone in southern Taiwan, *Radiat. Meas.*, 2008, vol. 43, pp. S348–S352.

Gol'din, S.V., Suvorov, V.D., Makarov, P.V., and Stefanov, Yu.P., An instability gravity model for the structure and stress-strain state of lithosphere in the Baikal Rift, *Rus. Geol. Geophys.*, 2006, vol. 46, no. 10, pp. 1079–1090.

Inceöz, M., Baykara, O., Aksoy, E., et al., Measurements of soil gas radon in active fault systems: a case study along the North and East Anatolian fault systems in Turkey, *Radiat. Meas.*, 2006, vol. 41, pp. 349–353.

Ioannides, K., Papachristodoulou, C., Stamoulis, K., et al., Soil gas radon: a tool for exploring active fault zones, *Appl. Radiat. Isot.*, 2003, vol. 59, pp. 205–213.

Karta noveishei tektoniki yuga Vostochnoi Sibiri. Masshtab 1 : 1 500 000 (The 1: 1500000 Neotectonic Map of the Southern Regions of East Siberia), Zolotarev, A.G. and Khrenov, P.M., Eds., Moscow: Mingeo SSSR, 1979.

Karta razlomov yuga Vostochnoi Sibiri. Masshtab 1 : 1500000 (The 1 : 1500000 Map of the Faults in the Southern Regions of East Siberia) Khrenov, P.M., Ed., Moscow: Mingeo SSSR, 1982.

Kemski, J., Klingel, R., and Siehl, A., Classification and mapping of radon-affected areas in Germany, *Environ. Int.*, 1996, vol. 22, Suppl. 1, pp. 789–798.

Khromovskikh, V.S., *Seismogeologiya Yuzhnogo Pribaikal'ya* (Seismogeology of the Southern Baikal Region), Moscow: Nauka, 1965.

King, C.-Y., Zhang, W., and King, B.-S., Radon anomalies on three kinds of faults in California, *Pure Appl. Geophys.*, 1993, vol. 141, no. 1, pp. 111–124.

Koike, K., Yoshinaga, T., and Asaue, H., Radon concentrations in soil gas, considering radioactive equilibrium conditions with application to estimating fault-zone geometry, *Environ. Geol.*, 2009, vol. 56, pp. 1533–1549.

Kompleks izmeritel'nyi dlya monitoringa radona "KAMERA-01". Rukovodstvo po ekspluatatsii (KAMERA-01 Radon Monitoring Complex: User Manual), Moscow: NITON, 2003.

Koval, P.V., Udodov, Yu.N., San'kov, V.A., Yasenovskii, A.A., and Andrulaitis, L.D., Geochemical activity of faults in the Baikal Rift Zone (mercury, radon, and rhoron), *Dokl. Earth. Sci.*, 2006, vol. 409A, no. 6, pp. 912–915.

Levi, K.G., Relative plate motion in the Baikal Rift Zone, *Geol. Geofiz.*, 1980, no. 5, pp. 9–15.

Lombardi, S. and Voltattorni, N., Rn, He and CO2 soil gas geochemistry for the study of active and inactive faults, *Appl. Geochem.*, 2010, vol. 25, pp. 1206–1220.

Mats, V.D., The structure and development of the Baikal rift depression, *Earth Sci. Rev.*, 1993, vol. 34, pp. 81–118.

Metodika ekspressnogo izmereniya ob"emnoi aktivnosti 222Rn v pochvennom vozdukhe s pomoshch'yu radiometra radona tipa RRA. Rekomendatsiya (Protocol of Express Measurements of Radon Activity in Soil by RPA Radon Radiometer. Guidelines), Moscow: NPP Doza, 2004.

Moussa, M.M. and El Arabi, A.-G.M., Soil radon survey for tracing active fault: a case study along Qena-Safaga road, Eastern Desert, Egypt, *Radiat. Meas.*, 2003, vol. 37, no. 3, pp. 211–216.

Palacky, G.J., Resistivity characteristics of geologic targets, in: *Electromagnetic Methods in Applied Geophysics*, Nabighian, M.N., Ed., Soc. Explor. Geophys., 1989, pp. 53–130.

Park, R.G., *Foundations of Structural Geology*, London: Chapman and Hall, 1997.

Popov, A.M., The results of deep magnetotelluric sounding in the Baikal region in the context of the data from other geophysical methods, *Izv. Akad. Nauk SSSR, Fiz. Zemli*, 1989, no. 8, pp. 31–37.

Richon, P., Klinger, Y., Tapponnier, P., et al., Measuring radon flux across active faults: relevance of excavating and possibility of satellite discharges, *Radiat. Meas.*, 2010, vol. 45, pp. 211–218.

Rikitake, T., Biosystem behaviour as an earthquake precursors, *Tectonophysics*, 1978, vol. 51, pp. 1–20.

San'kov, V.A., Miroshnichenko, A.I., Levi, K.G., et al., Cenozoic stress field evolution in the Baikal rift zone, *Bull. Cent. Rech. Elf Explor. Prod.*, 1997, vol. 21, no. 2, pp. 435–455.

San'kov, V.A., Lukhnev, A.V., Miroshnichenko, A.I., Ashurkov, S.V.,?Byzov, L.M., Dembelov, M.G., Calais, E., and Déverchère,?J., Extension in the Baikal Rift: present-day kinematics of passive rifting, *Dokl. Earth Sci.*, 2009, vol. 425, no. 2, pp. 205–209.

Seminsky, K.Zh., *Vnutrennyaya struktura kontinental'nykh razlomnykh zon. Tektonofizicheskii aspekt* (Internal Structure of Continental Fault Zones: Tectonophysical Aspect), Novosibirsk: SO RAN, GEOS, 2003.

Seminsky, K.Zh. and Bobrov, A.A., Radon activity of faults (western Baikal and southern Angara areas), *Rus. Geol. Geophys.*, 2009a, vol. 50, no. 8, pp. 682–692.

Seminsky, K.Zh. and Bobrov, A.A., Comparative assessment of radon activity for different fault types and scale ranks in the Baikal Rift and south of the Siberian Platform, *Dokl. Earth Sci.*, 2009b, vol. 427A, no. 6, pp. 915–919.

Seminsky, K.Zh. and Radziminovich, Ya.B., Cross-sectional sizes and lateral zonality of the Baikal Seismic Belt, *Dokl. Earth Sci.*, 2011, vol. 438, part 1, pp. 645–648.

Seminsky, K.Zh. and Bobrov, A.A., The first results of studies of temporary variations in soil-radon activity of faults in Western Pribaikalie, *Geodinam. Tektonofiz.*, 2013, vol. 4, no. 1, pp. 1–12.

Seminsky, K.Zh. and Demberel, S., The first estimations of soil-radon activity near faults in Central Mongolia, *Radiat. Meas.*, 2013, vol. 49, pp. 19–34.

Seminsky, K.Zh., Kozhevnikov, N.O., Cheremnykh, A.V., Pospeeva, E.V., Bobrov, A.A., Olenchenko, V.V., Tugarina, M.A., Potapov, V.V., Zaripov, R.M., and Cheremnykh, A.S., Interblock zones in the crust of the southern regions of East Siberia: tectonophysical interpretation of geological and geophysical data, *Geodinam. Tektonofiz.* 2013, vol. 4, no. 3, pp. 203–278.

Spivak, A.A., The specific features of geophysical fields in the fault zones, *Izv., Phys. Solid Earth*, 2010, vol. 46, no. 4, pp. 327–338.

Sun, Yunshen, Krylov, S.V., Baojiun, Yan, et al., Deep seismic sounding of the lithosphere on Baikal–Northeast China international transect, *Geol. Geofiz.*, 1996, vol. 37, no. 2, pp. 3–15.

Suvorov, V.D. and Tubanov, Ts.A., Distribution of local earthquakes in the crust beneath central Lake Baikal, *Rus. Geol. Geophys.*, 2008, vol. 49, no. 8, pp. 611–620.

Tansi, C., Tallarico, A., Iovine, G., et al., Interpretation of radon anomalies in seismotectonic and tectonic-gravitational settings: the south-eastern Crati graben (Northern Calabria, Italy), *Tectonophysics*, 2005, vol. 396, pp. 181–193.

Toutain, J.-P. and Baubron, J.-C., Gas geochemistry and seismotectonics: a review, *Tectonophysics*, 1999, vol. 304, pp. 1–27.

Utkin, V.I., Mamyrov, E., Kan, M.V., Krivasheev, S.V., Yurkov, A.K., Kosyakin, I.I., and Shishkanov, A.N., Radon monitoring in the Northern Tien Shan with application to the process of tectonic earthquake nucleation, *Izv., Phys. Solid Earth*, 2006, vol. 42, no. 9, pp. 775–784.

Voitov, G.I., Monitoring the radon activity in subsoil air seismically active Central Asia, *Izv. Akad. Nauk, Fiz. Zemli*, 1998, no. 1, pp. 27–38.

Walia, V., Mahajan, S., Kumar, A., et al., Fault delineation study using soil-gas method in the Dharamsala area, NW Himalayas, India, *Radiat. Meas.*, 2008, vol. 43, pp. S337–S342.

Walia, V., Lin, S.J., Fu, C.C., et al., Soil-gas monitoring: a tool for fault delineation studies along Hsinhua Fault (Tainan), Southern Taiwan, *Appl. Geochem.*, 2010, vol. 25, pp. 602–607.

Wiersberg, N. and Erzinger, J., Origin and spatial distribution of gas at seismogenic depths of the San Andreas fault from drill-mud gas analysis, *Appl. Geochem.*, 2008, vol. 23, pp. 1675–1690.

Translated by M. Nazarenko